Plant Physiology and Biochemistry 136 (2019) 13–21

Contents lists available at ScienceDirect

Plant Physiology and Biochemistry

journal homepage: www.elsevier.com/locate/plaphy

Research article

Slower development of PSI activity limits photosynthesis during *Euonymus japonicus* leaf development

Xin Zhong[a,b], Xingkai Che[a,c], Zishan Zhang[a,c], Shuhao Li[a,b], Qingming Li[a,b,d,*], Yuting Li[a,c,**], Huiyuan Gao[a,c]

[a] State Key Laboratory of Crop Biology, Shandong Agricultural University, Tai'an, Shandong, 271018, China
[b] College of Horticulture Science and Engineering, Shandong Agricultural University, Tai'an, Shandong, 271018, China
[c] College of Life Sciences, Shandong Agricultural University, Tai'an, Shandong, 271018, China
[d] Scientific Observing and Experimental Station of Environment Controlled Agricultural Engineering in Huang-Huai-Hai Region, Ministry of Agriculture, Tai'an, 271018, China

ARTICLE INFO

Keywords:
Development of *Euonymus japonicus*
PSI and PSII
Photosynthetic core protein
Fluorescence transient
Photosynthetic electron transport
RuBP regeneration

ABSTRACT

This study primarily explored the limiting factor for photosynthesis during the development of *Euonymus japonicus* leaves. The analysis of the chlorophyll fluorescence transient, pulse-modulated fluorescence, 820-nm reflection, and expression of core proteins for photosystems demonstrated that photosystem II (PSII) activity developed more rapidly than did photosystem I (PSI) activity. The slower development of the PSI activity restricted linear and cyclic electron transport and thus inhibited the production of ATP and NADPH, which inhibits the activation of Rubisco, resulting in low activity of carboxylation efficiency. The application of exogenous NADPH (50 μM) and ATP (100 μM) to leaves remarkably increased the P_n and *CE* in the youngest leaf but not in the fully expanded leaf, which indicated that an inadequate supply of the assimilatory power significantly inhibited *CE* and P_n. We concluded that the slower development of the PSI activity was one of the most important limiting factors for photosynthesis during the development of *E. japonicus* leaves.

1. Introduction

Photosynthesis in plants consists of light reactions and dark reactions. The light reactions involve the cooperation of two photosystems, i.e., photosystem I(PSI) and photosystem II (PSII), of which the main function is the absorption and conversion of light to provide assimilatory power (adenosine-triphosphate, ATP; and reduced form of nicotinamide-adenine dinucleotide phosphate, NADPH) for the dark reaction (i.e., the Calvin cycle). The dark reactions consist of several enzymatic reactions, which use the assimilatory power produced by the light reactions to assimilate CO_2 into carbohydrates. To optimize normal photosynthesis, the photosynthetic components, including PSI, PSII, and the Calvin cycle, must smoothly operate in coordination. Under stress conditions, the inhibition of any step will affect the overall photosynthesis (Brestic et al., 2015; Çiçek et al. 2018).

Euonymus japonicus is one of the most popular evergreen tree species cultivated in cities of central and northern China. One of the species' notable characteristics is that newly formed shoots grow rapidly during late March and early April. New shoots are formed within approximately two weeks; additionally, there are leaves from fully expanded to newly initiated leaves on the new shoots. Therefore, the species provides excellent material to study the development of photosynthesis in the leaves of a woody plant, and the use of this species avoids the influence of great fluctuations in environmental conditions on leaf development due to the long developmental period required to form leaves at different developmental stages for other plants.

During leaf development, not only does the leaf area change significantly, but the structure and function of the leaf photosynthetic apparatus also gradually improve (Bongi et al., 1987; Maayan et al., 2008; Gao et al., 2014). With leaf expansion, the chlorophyll content (Chl), stomatal conductance (G_s), photosynthetic rate (P_n), carboxylation efficiency (*CE*), activity of PSI and PSII, and CO_2 assimilation rate also increase(Bertamini and Nedunchezhian, 2002; Jiang et al., 2006a; Maayan et al., 2008). It has been suggested that PSI and PSII co-develop and that PSII is not a limiting factor during the development of grape leaves (Jiang et al., 2006a). Maayan et al. (2008) reported that the

* Corresponding author. College of Horticulture Science and Engineering, Shandong Agricultural University, Tai'an, Shandong, 271018, China.
** Corresponding author. College of Life Sciences, Shandong Agricultural University, Tai'an, Shandong, 271018, China.
E-mail addresses: 751538948@qq.com (X. Zhong), chexingkai@163.com (X. Che), zhangzishantaian@163.com (Z. Zhang), 762547422@qq.com (S. Li), gslqm@sdau.edu.cn (Q. Li), liyuting0531@163.com (Y. Li), gaohy@sdau.edu.cn (H. Gao).

https://doi.org/10.1016/j.plaphy.2019.01.004
Received 2 October 2018; Received in revised form 3 January 2019; Accepted 3 January 2019
Available online 04 January 2019
0981-9428/

Abbreviations

ATP	adenosine triphosphate
Chl	chlorophyll content
C_i	intercellular CO_2 concentration
G_s	stomatal conductance
ETR	linear electron transport rate
F_m	maximum fluorescence
F_m'	maximum fluorescence in the light-adapted state
F_m-F_o	maximum variable fluorescence of PSII
F_o	minimal fluorescence
F_o'	minimum fluorescence in the light-adapted state
F_s	steady-state fluorescence
F_v/F_m	maximum PSII photochemical efficiency
F_v'/F_m'	maximum PSII photochemistry efficiency in light adapted leaf
$\triangle I/I_o$	relative content of active P700
NADPH	triphosphopyridine nucleotide
OEC	oxygen-evolving complex
OJIP curve	chlorophyll *a* fluorescence transient
PET	photosynthetic electron transport
P_n	photosynthetic rate
PSI	photosynthesis system I
PSII	photosynthesis system II
Φ_{PSII}	actual quantum yield of PSII photochemistry
q_P	open degree of PSII reaction centers
Rubisco	ribulose-1,5-bisphosphate carboxylase/oxygenase
RuBP	ribulose-1,5-bisphosphate
RC/CS_o	active reaction centers per leaf cross-section
Ψ_o	probability that a trapped exciton moves an electron into the electron transport chain beyond Q_A^-

developmental rate of the Calvin cycle is slower than that of the light reactions.

However, comprehensive and systematic studies on the developmental rates of the PSI, PSII, and Calvin cycle during the development of *E. japonicus* leaves are lacking. Although Maayan et al. (2008) observed that the core proteins of the PSII and the Calvin cycle increased in abundance with leaf development, the relationship between the expression of photosynthetic core proteins and the activity of each step of the photosynthetic apparatus was not analyzed. The supply and demand of assimilatory power between the light reactions and dark reactions during leaf development is also an important factor affecting photosynthesis; however, until now, it has not been explored.

The present study aimed to determine which developmental step is a limiting factor for photosynthesis and to clarify the relationship between the light reactions and dark reactions during leaf development in *E. japonicus*. The research will improve our understanding of the limiting factors of P_n during the development of the photosynthetic apparatus of a plant.

2. Materials and methods

2.1. Plant materials

Experiments were conducted in Tai'an, Shandong Province, China, in late March and early April in 2017 and 2018. Plants of *E. japonicas* were grown in a loamy soil field, where nutrients and water were supplied sufficiently throughout the experiment to prevent potential nutrient and drought stresses. The *E. japonicus* grew outside in the natural condition. The maximum light intensity around noon time was about 1400 μmol $m^{-2}.s^{-1}$ during the growing period of the new shoots, and it became completely dark after sun set, the light intensity had a diurnal change during day time. The temperature, during the growing period of the new shoots, ranged from 17 to 28 °C during day time and 9–17 °C during night time, respectively. The light and temperature ranges during the growing period of the new shoots (about 2 weeks) did not change obviously. The first four nodes from the apical portion of the new shoots on the south-facing side of the plants were selected for the experiment.

2.2. Leaf area and Chl

The leaf area was measured with a portable scanning planimeter (CI-202, CID Bio-Science, Camas, Washington, USA). The leaf area of a fully developed leaf was considered to be 100%, while the leaf area of immature leaves was determined as the percentage of that of a fully developed leaf.

For the determination of leaf Chl, leaves at different developmental stages were cut into 0.44 cm^2 discs. Eight leaf discs were placed in a test tube containing 10 mL of 80% acetone, incubated in the dark at 25 °C, and then extracted for 48 h. Three replications were performed per developmental stage. The absorbance of the extracts was measured using an ultraviolet–visible spectrophotometer (UV-1601, Shimadzu, Japan) in accordance with the method described in Porra (2002).

2.3. Chlorophyll a fluorescence transient

The chlorophyll *a* fluorescence transient (the O-J-I-P curve) was measured using an M-PEA fluorometer (Hansatech, King's Lynn, UK).Saturating red light (5000 μmol $m^{-2}s^{-1}$) was produced by an array of four light-emitting diodes (LED; peak wavelength 650 nm). All leaves were dark-adapted at room temperature (25 °C) for 30 min. The chlorophyll *a* fluorescence transients were measured by exposure to a 1-s pulse of saturating red light. The data were analyzed using the JIP-test (Strasser et al., 2000). The JIP-test parameters were calculated according to Maxwell and Johnson (2000):

(1) Maximum variable fluorescence of PSII: $F_m - F_o$, where F_m is the maximum chlorophyll fluorescence, and F_o is the minimum chlorophyll fluorescence;
(2) Maximum PSII photochemical efficiency: $F_v/F_m = 1 - (F_o/F_m)$, where F_v is the variable chlorophyll fluorescence;
(3) Probability that a trapped exciton moves an electron into the electron transport chain beyond Q_A^-: $\Psi_o = 1 - V_J$, where Q_A^- is the primary quinone acceptor of PSII, and V_J is the value of the fluorescence at point J.
(4) Active reaction centers per leaf cross-section: $RC/CS_o = (F_v/F_m)\cdot(V_J/M_o)\cdot(ABS/CS_o)$.

2.4. Pulse-modulated chlorophyll fluorescence

Pulse-modulated chlorophyll fluorescence was measured using a FMS-2 pulse-modulated fluorometer (Hansatech) according to Jia et al. (2010). All leaves were dark-adapted for 30 min before measurements were taken. The F_o was measured using weak modulated light. A 0.8-s pulse of saturating light of approximately 8000 μmol $m^{-2}s^{-1}$ was used to measure F_m. Then, the leaf was illuminated by an actinic light of approximately 800 μmol $m^{-2}s^{-1}$. The steady-state fluorescence (F_s) was recorded, then a 0.8-s pulse of saturating light of approximately 8000 μmol $m^{-2}s^{-1}$ was applied to measure the maximum fluorescence under light (F_m'). The actinic light was then switched off, and the minimum fluorescence under light (F_o') was determined after illumination with far-red light for 3 s.

The following parameters were calculated in accordance with Maxwell and Johnson (2000).

(1) Open degree of PSII reaction centers: $q_P = (F_m' - F_s)/(F_m' - F_o')$;
(2) Actual quantum yield of PSII photochemistry: $\Phi_{PSII} = 1 - F_s/F_m' = q_P * F_v'/F_m'$
(3) Linear electron transport rate (ETR) = Φ_{PSII}*PPFD*0.5*0.83, where PPFD is the actinic photon flux density, 0.83 is the coefficient of leaf absorption, and 0.5 represents an equal distribution between PSI and PSII.
(4) The maximum PSII photochemistry efficiency under light: $F_v'/F_m' = (F_m' - F_o')/F_m'$.

2.5. Measurement of 820-nm reflection curves of leaves

The measurement method was performed according to (Salvatori et al., 2014). Measurements of 820-nm reflection were performed using an M-PEA fluorometer (Hansatech). At the time of 0 s, a dark-adapted leaf was illuminated with far-red light (approximately 100 μmol $m^{-2} s^{-1}$) until steady P700 photo-oxidation was attained (i.e., at time 20 s); then, the far-red light was stopped. A modulated (33.3 kHz) measuring light at 820 nm was provided simultaneously with the illumination of far-red light. The change in amplitude of the 820-nm reflection ($\Delta I/I_o$) was calculated and used to compare the relative content of active P700 (Kim et al., 2001; Zhang et al., 2011). The following formula was used to calculate $\Delta I/I_o$: $\Delta I/I_o = (I_o - I_m)/I_o$, where I_o is the initial 820-nm reflection signal between 0.4 and 10 ms, and I_m is the minimum 820-nm reflection signal under far-red illumination.

2.6. Gas exchange in leaves

P_n, G_s, and C_i were measured with a CIRAS-3 portable photosynthesis system (PP Systems, Haverhill, Mass., USA) under saturated PPFD (1200 μmol $m^{-2} s^{-1}$ light intensity), 400 μmol mol^{-1} CO_2, and 60% relative humidity at 25 °C; these conditions were regulated by the CIRAS-3control system. The measurement method was performed according to Jin et al. (2017). The P_n–C_i response curves were measured at 25 °C. We used the light source of CIRAS-3 photosynthesis system to adapt the leaves under measuring light intensity for 15–20 min, and the parameters were recorded until the plants were fully adapted to the light. The CO_2 concentration was changed every 3 min in a sequence of 400, 300, 200, 100, 400, 600, 800, 1000, 1200, 1400, 1600, 1800, and 2000 μmol mol^{-1}, which was enabled by the use of a CO_2 supply system of the CIRAS-3. *CE* was calculated according to the initial slope of the P_n–C_i response curve. From the response curves, we also derived the ribulose 1,5-bisphosphate (RuBP) maximum regeneration rate, which was the maximum P_n under a saturated CO_2 concentration and saturated light (Farquhar et al., 1980). Each measurement was repeated three times with an independent leaf. The P_n and P_n–C_i response curves were measured between 08:00 and 11:30 on sunny days. After measuring the gas exchange, the leaves were placed in liquid nitrogen for analysis using Western blotting.

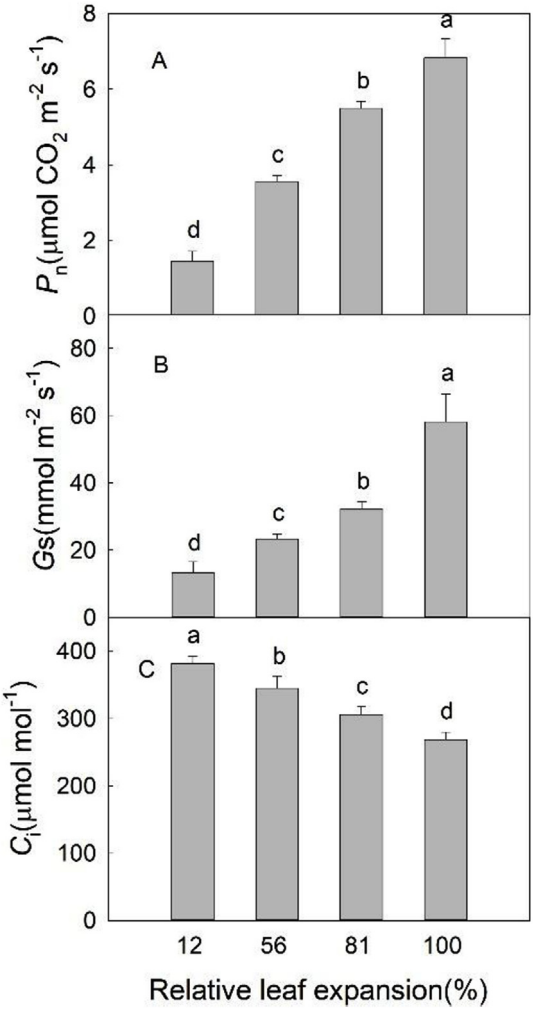

Fig. 2. Changes in P_n (A), G_s (B) and C_i (C) in different expanded leaves. Different letters in the data column indicate significant differences ($p < 0.05$).

To examine the effect of exogenous assimilatory power on photosynthesis, before treatment, we tested a concentration gradient series of ATP and NADPH to select a suitable working concentration (100 μM ATP and 50 μM NADPH) that represented the optimal concentration for

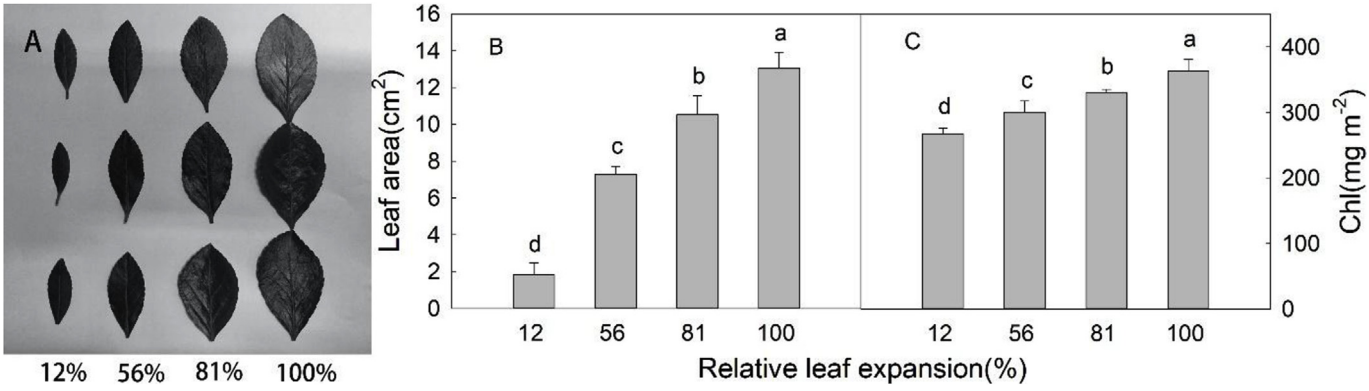

Fig. 1. Changes in leaf area (A, B) and chlorophyll content(C) in different expanded leaves. The newly fully expanded leaves were considered to be 100%, while the values of other expanded leaves were based on the percentage of the fully expanded leaves. This information applies to all Figures in this article. Different letters in the data column indicate significant differences ($p < 0.05$).

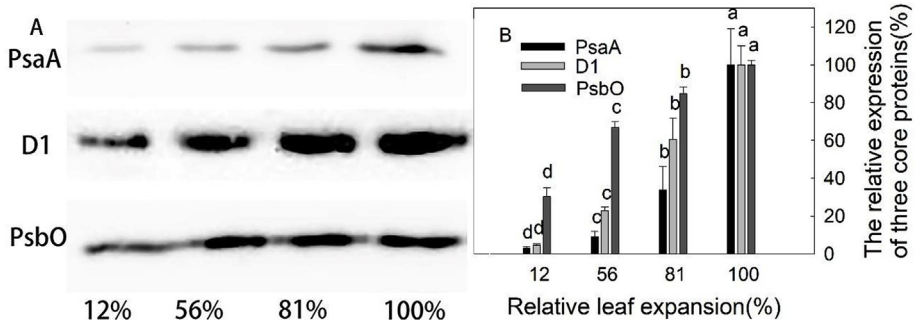

Fig. 3. The expression of the PSI core protein (PsaA), PSII core protein (D1), and oxygen evolving complex core protein (PsbO) in different expanded leaves (A). The relative expression of the three core proteins in different expanded leaves (B). The different letters in Fig 3B indicate significant differences ($p < 0.05$) between the same proteins of different expanded leaves. Different letters in the data column indicate significant differences ($p < 0.05$).

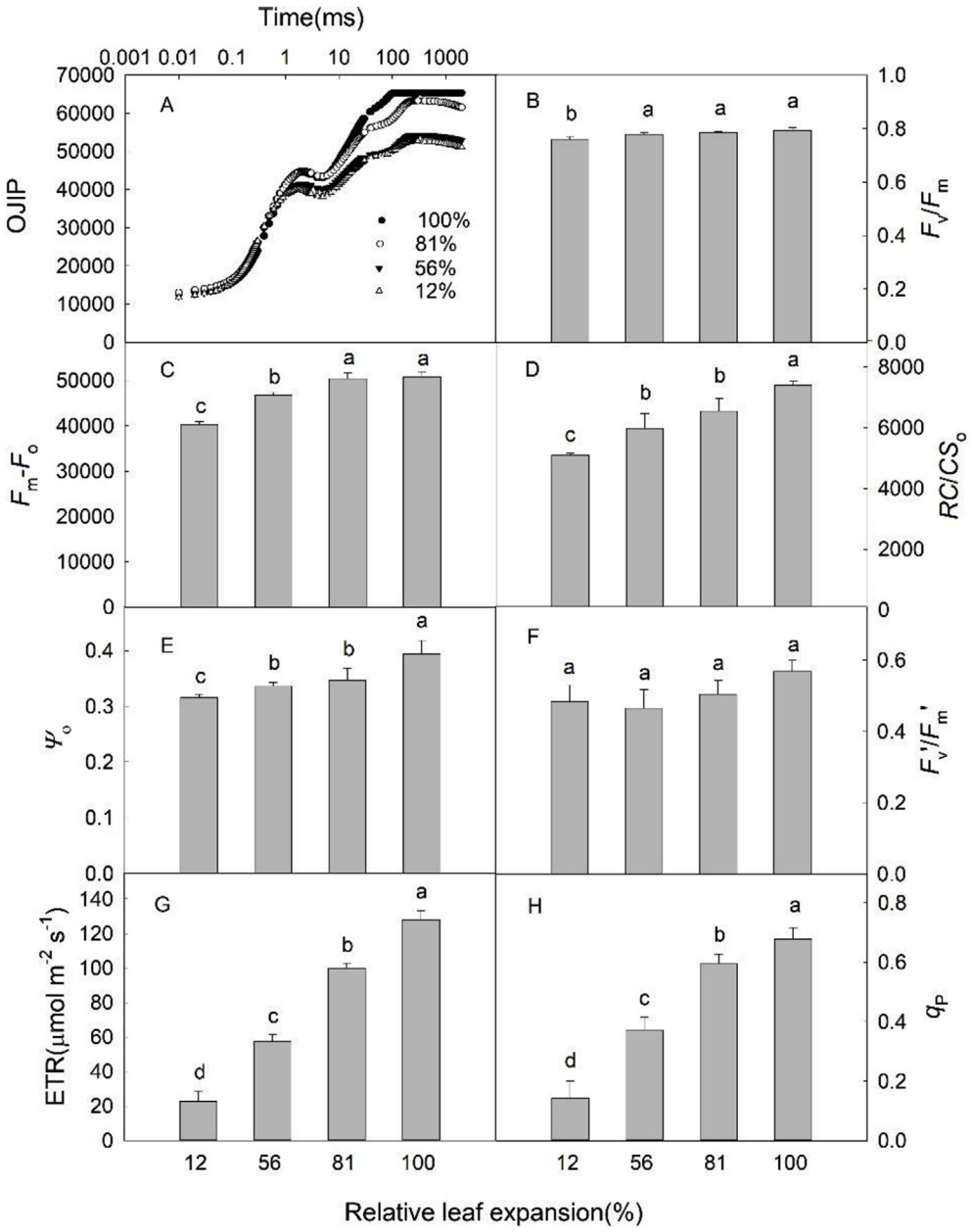

Fig. 4. Chlorophyll fluorescence transient of different expanded leaves (A) and the parameters obtained from the JIP-test. The maximum photochemical efficiency of PSII, F_v/F_m (B), the maximum variable PSII photochemical activity, F_m-F_o (C), the number of active reaction centers per cross-section of leaf, RC/CS_o (D), the probability that a trapped exciton moves an electron into the electron transport chain beyond Q_A^-, Ψ_o (E), the maximum PSII photochemistry efficiency under light, F_v'/F_m' (F), the linear electron transport rate, ETR (G), and the open degree of PSII reaction center, q_P (H) in different expanded leaves. Different letters in the data column indicate significant differences ($p < 0.05$).

enhancing photosynthesis. Many previous studies have reported that the application of exogenous ATP and NADPH affects plants, which indicates that the exogenous ATP and NADPH can enter the chloroplasts (Tanaka et al., 2010; Tonón et al., 2010). In the present study, the treatment was performed as follows. Newly developed shoots were excised at the base, and the basal portion was inserted into a solution of 100 μM ATP and 50 μM NADPH. The control shoots were inserted in water. The basal portion (approximately 1 cm) of all shoots was cut in the solution or water to maintain normal water absorption and transportation. The shoots were incubated under 600 μmol m^{-2} s^{-1}PPFD at 25 °C. After 1 h, approximately 1.5 mL of the solution was absorbed by each shoot via transpiration during the treatment period. Then, P_n was

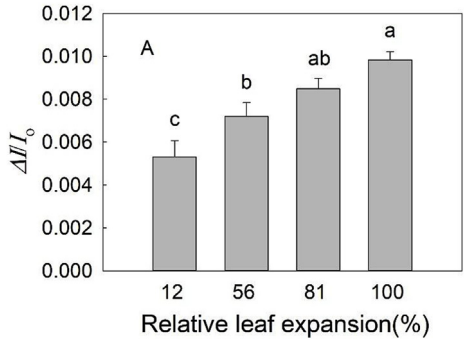

Fig. 5. The content of active P700, $^{\triangle}I/I_o$. Different letters in the data column indicate significant differences ($p < 0.05$).

measured under saturated light (1200 μmol $m^{-2} s^{-1}$) at 400 μmol mol^{-1} CO_2 and 25 °C.

2.7. Western blotting

The method for Western blotting was based on the method used in Mahmood and Yang. (2012); specifically, the thylakoid membrane proteins, such as the PSI core protein (PsaA), the PSII core protein (D1), the OEC core protein (PsbO), and the soluble protein ribulose-1,5-bisphosphate carboxylase/oxygenase (Rubisco, EC4.1.1.39), which is a core protein of the Calvin cycle, were detected by Western blotting. To prepare the thylakoid membrane proteins, leaf fragments were homogenized in ice-cold grinding buffer containing 0.4 M sorbitol, 5 mM EDTA, 5 mM $MgCl_2$, 10 mM $NaHCO_3$, 20 mM Tricine/NaOH (pH 8.4), and 0.5% (w/v) fatty acid-free bovine serum albumin (BSA). The homogenate was filtered through four layers of cheesecloth, and then the suspension was centrifuged at 3000 *g* for 5 min at 4 °C. The sediments were washed with 2 mL resuspension buffer containing 0.3 M sorbitol, 2.5 mM EDTA, 5 mM $MgCl_2$, 10 mM $NaHCO_3$, 20 mM HEPES/KOH (pH 7.8), and 0.5% (w/v) fatty acid-free BSA and then centrifuged at 3000 *g* for 5 min at 4 °C. The sediment was re-suspended in 1 mL hypotonic buffer containing 2.5 mM EDTA, 5 mM $MgCl_2$, 10 mM $NaHCO_3$, 20 mM HEPES/KOH (pH 7.8), and 0.5% (w/v) fatty acid-free BSA. The resuspension was adjusted to a final volume of 5 mL with hypotonic buffer. After 5 min, the solution was centrifuged at 50000 *g* for 10 min at 4 °C. The supernatant was carefully discarded, and the pellet was finally suspended in resuspension buffer for Western blotting. For the soluble protein Rubisco, samples (0.2 g) were solubilized in 2 mL grinding buffer and centrifuged at 3000 *g* for 5 min. The supernatant was used for Western blotting. The membrane proteins and the soluble protein were denatured by boiling in loading buffer containing SDS, and then 10 μL of the extracts (25 μg protein) was loaded onto the top of the gel and separated by 12% polyacrylamide gradient gel electrophoresis. The isolated proteins in the gel were electro-blotted onto PVDF membranes, probed with an antibody, and visualized using the enhanced chemiluminescence method. The quantitative image analysis of the protein levels was performed with Gel-Pro Analyzer 4.0 software. The antibodies for the four core proteins were purchased from Agrisera Company (Sweden).

2.8. Assay of electron transport activities

The measurement method was performed according to that described in Jin et al. (2017).Samples (1 g) of leaves that were at different developmental stages were floated on ice-cold water for 30 min in the dark. All subsequent steps were performed in the dark at 4 °C, and all of the equipment and buffers that were used were pre-cooled. The leaves were rapidly homogenized with a mortar and pestle in 5 mL grinding buffer containing 0.4 M sorbitol, 5 mM EDTA, 5 mM $MgCl_2$, 10 mM $NaHCO_3$, 20 mM Tricine/NaOH (pH 8.4), and 0.5% (w/v) fatty acid-free BSA. The homogenate was filtered through four layers of cold-water-soaked cheesecloth. The suspension was centrifuged at 300 *g*for 3 min to remove coarse matter and then at 3000 *g* for 3 min at 4 °C. The supernatant was carefully discarded, and the pellet was suspended in 2 mL resuspension buffer containing 0.3 M sorbitol, 2.5 mM EDTA, 5 mM $MgCl_2$, 10 mM $NaHCO_3$, 20 mM HEPES/KOH (pH 7.8), and 0.5% (w/v) fatty acid-free BSA; finally, the sample was centrifuged at 3000 *g* for 3 min at 4 °C. The pellet was re-suspended in 1 mL hypotonic buffer containing 2.5 mM EDTA, 5 mM $MgCl_2$, 10 mM $NaHCO_3$, 20 mM HEPES/KOH (pH 7.8), and 0.5% (w/v) fatty acid-free BSA. The resuspension was adjusted to a final volume of 5 mL with hypotonic buffer and then put aside for 5 min. The thylakoid membranes were collected by centrifugation at 3000*g* for 5 min at 4 °C. Finally, the pellet was re-suspended in 1.0 mL resuspension buffer, and the suspension was stored on ice in the dark until use. One of each of the thylakoid membrane preparations was used to measure the leaf chlorophyll content. The other thylakoid membrane preparations were used to assay electron transport activities using the Oxytherm oxygen electrode system (Hansatech). The PSII activity was determined by O_2 evolution with 1 mM*p*-benzoquinone as an electron acceptor (Satoh et al., 1992). The PSI activity was measured as the O_2 uptake in the presence of 0.1 mM 2,6-dichlorophenol indophenol, 0.1 mM methylviologen (MV), 5 mM NaN_3 as an inhibitor of respiration, 10 μM 3-(3,4-dichlorophenyl)-1,1-dimethylureaas an inhibitor of PSII, and 5 mM ascorbate as an inhibitor of superoxide dismutase (Brandle et al., 1977).

After adjusting the Oxytherm oxygen electrode (Hansatach, UK), 1.8 mL buffer (50 mM HEPES-KOH (pH 7.6), 100 mM sorbitol, 10 mM KCl, 10 mM $MgCl_2$, 5 mM NH_4Cl), and 200 μL chloroplast extraction were added to the reaction cup. The PSII activity was calculated according to the upward slope of the O_2 curve under saturated light (10 000 μmol $m^{-2} s^{-1}$) by adding 50 μL 1 mM p-benzoquinone as an electron acceptor to the reaction cup (Satoh et al., 1992). The PSI activity was calculated according to the downward slope of the O_2 curve by adding 10 μL 0.1 mM 2,6-dichlorophenol indophenol, 10 μL 0.1 mM MV, 10 μL 5 mM NaN_3 as an inhibitor of respiration, 10 μL 10 μM 3-(3,4-dichlorophenyl)-1,1-dimethylurea as an inhibitor of PSII, and 10 μL 5 mM ascorbate as an inhibitor of superoxide dismutase to the reaction cup.

2.9. Statistical analysis

All measurements were repeated at least three times using independent leaves unless otherwise stated. Standard deviations were calculated using Excel software (Microsoft, Redmond WA, USA). Least significant differences were calculated using SPSS 11 software (SPSS

Table 1
The photosynthetic electron transport activities (μmol O_2 h^{-1} mg^{-1}Chl) in different expanded leaves of *E. japonicus*.

Electron transport activity	O_2 evolution/uptake (μmol O_2 h^{-1} mg^{-1}Chl)			
	12% leaf area	56% leaf area	81% leaf area	100% leaf area
PSII (H_2O→*p*-BQ)	102.0 ± 7.2^{b}	153.9 ± 18.9^{a}	155.4 ± 14.4^{a}	163.6 ± 17.5^{a}
Relative O_2 evolution	62.3%	94.0%	94.9%	100%
PSI (DCPIPH_2→MV)	250.4 ± 18.1^{d}	336.8 ± 10.3^{c}	450.9 ± 14.4^{b}	531.4 ± 56.7^{a}
Relative O_2 uptake	47.1%	63.4%	84.9%	100%

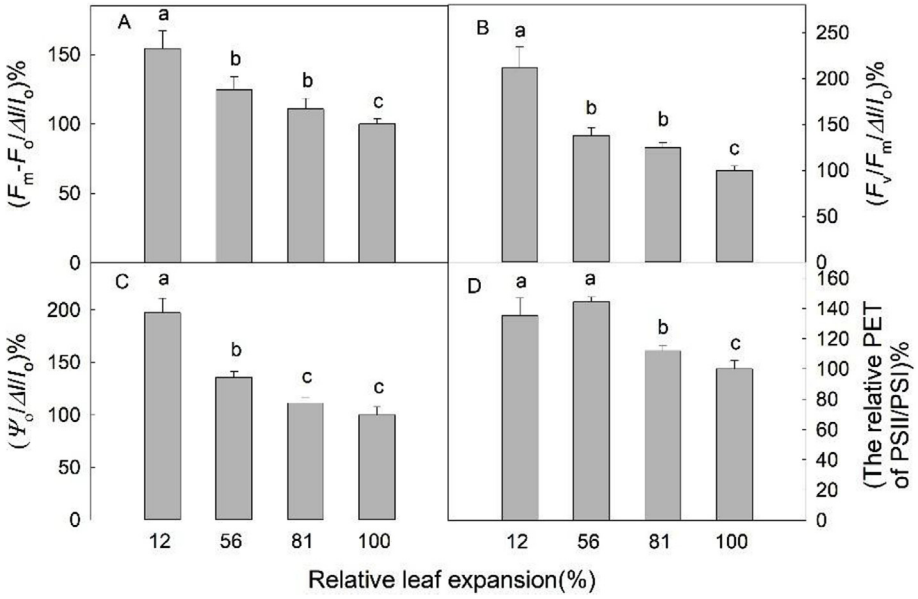

Fig. 6. Changes in the ratio of PSII activity to PSI activity, $(F_m\text{-}F_o/\Delta I/I_o)\%$ (A),$(F_v/F_m/\Delta I/I_o)\%$ (B),$(\Psi_o/\Delta I/I_o)\%$ (C), the ratio of photosynthetic electron transport(PET) activities of PSI to PSII(D) in the different expanded leaves of *E. japonicus*. The activities of PSI and PSII in fully expanded leaves were considered to be 100%, while those of other leaves were -determined based on the percentage of that in fully expanded leaves. Different letters in the data column indicate significant differences ($p < 0.05$).

Inc., Chicago, IL, USA) to analyze the differences in the measured parameters between leaves at different developmental stages.

3. Results

3.1. Leaf area, chlorophyll content, and photosynthesis parameters during leaf development

The leaf area and chlorophyll content gradually increased with leaf expansion (Fig. 1), which implied that the capability for light-energy absorption increased with leaf development. Additionally, with leaf expansion, G_s and P_n increased significantly, while C_i decreased significantly (Fig. 2).

3.2. Expression of light-reaction core proteins

The expression of core proteins in the light reactions gradually increased with leaf development. Given that the photosynthetic apparatus is composed of different concentrations of various proteins, it was impractical to compare the absolute content of each protein to reflect the extent of development of different complexes of the photosynthetic apparatus. Therefore, the relative expression level of the different proteins objectively reflected the relative developmental rate of the different complexes of the photosynthetic apparatus. The ratio of the expression of PsaA, D1, and PsbO in the youngest leaves to that in the fully expanded leaves was 3.04%, 6.1%, and 25.6%, respectively (Fig. 3).

3.3. Activity of PSII

The present results demonstrated that the chlorophyll fluorescence transients changed considerably with leaf expansion (Fig. 4A). The maximum variable fluorescence of PSII ($F_m - F_o$), the maximum photochemical efficiency of PSII (F_v/F_m), the number of active reaction centers per cross-section of leaf area (RC/CS_o), and the probability that a trapped exciton moves an electron into the electron transport chain beyond Q_A^- (Ψ_o) all increased slightly during leaf development. The ETR and the open degree of the PSII reaction centers (q_P) increased markedly, while the maximum PSII photochemistry efficiency in light-adapted leaves (F_v'/F_m')was not significantly different in leaves at different stages of development (Fig. 4).

3.4. Activity of PSI

In the present study, the content of active P700 in the youngest leaf was much lower than that in leaves at the other three developmental stages that were examined (Fig. 5).

3.5. Differences in PSI and PSII activities

In Table 1, different letters in the same line indicate significant differences among different expanded leaves ($p < 0.05$). Values are means ± SD ($n = 3$).

In addition to analyzing the fluorescence parameters, we also assayed the PSII and PSI electron transport rate by analyzing O_2 evolution/uptake using an oxygen electrode system. The PSI electron transport activity increased markedly with leaf development, while the PSII electron transport rate was almost identical to that in the mature leaf when the leaf area attained a value of 56% of the fully expanded leaf (Table 1).

To clarify the relative development rates of PSI and PSII during leaf expansion, the relative activities of PSI and PSII were compared (Fig. 6). From the youngest leaves to the fully expanded leaves, the activities of PSI and PSII increased. In the youngest leaf, the PSII activity was much higher than was the PSI activity.

3.6. P_n–C_i response curve, CE, RuBP maximum regeneration, and Rubisco expression

Marked differences in the P_n–C_i response curves were observed at different stages of leaf expansion. The P_n in the youngest leaf increased only slightly (i.e., by approximately 2.5 μmol (CO_2) $m^{-2}s^{-1}$) with increasing CO_2 concentration, while that of the fully expanded leaf increased substantially more (i.e., by approximately 17 μmol (CO_2) $m^{-2}s^{-1}$) with increasing CO_2 concentration. The relative expression level of Rubisco in the youngest leaf was approximately 25% of that in the fully expanded leaf, and the expression percentage was much higher than those of the PSI and PSII core proteins. However, the *CE* and RuBP maximum regeneration rate were both remarkably lower in the youngest leaves than in the fully expanded leaves, and the ratios of the *CE* and RuBP maximum regeneration rate in the young leaf to the fully expanded leaf was much lower than were the ratios of the PSI and PSII activities in the young leaf to the fully expanded leaf (Figs. 4, 5 and 7).

The abovementioned results indicated that the relative activity of

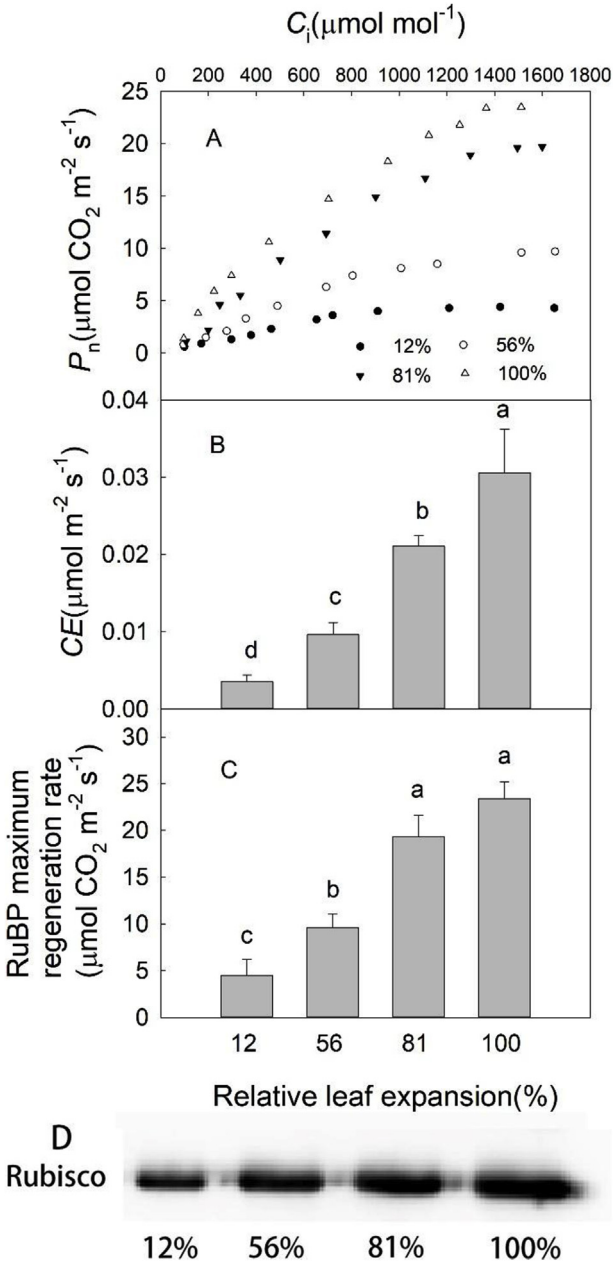

Fig. 7. Changes in the P_n-Ci response curve (A), carboxylation efficiency (B), RuBP maximum regeneration rate (C) and expression of Rubisco (D) in *E. japonicas* leaves at different stages of development. Different letters in the data column indicate significant differences ($p < 0.05$).

PSII was higher than that of PSI in young leaves. This characteristic will limit the electron transport rate in young leaves, which in turn, limits the formation of assimilatory power and further inhibits the dark reactions.

3.7. Effect of exogenous assimilatory power on photosynthetic CO_2 fixation

To investigate whether the relationship between the light reactions and dark reactions was associated with assimilatory power (ATP and NADPH) and whether the low activity of the dark reactions in young leaves was correlated with the low activity of PSI, we applied exogenous assimilatory power (100 μM ATP and 50 μM NADPH) to the youngest and fully expanded leaves. The results showed that 1 h after treatment, the P_n and *CE* in the youngest leaves increased by approximately 50%, while the treatments had no observable influence on these photosynthetic parameters in the fully expanded leaves (Fig. 8). These results verified that the supply of an insufficient quantity of assimilatory power caused by the low capacity for electron transport in young leaves greatly limited the P_n.

4. Discussion

Photosynthetic CO_2 fixation by leaves depends on coordination between light reactions and dark reactions. Our results demonstrated that during *E. japonicas* leaf development, the lower PSI activity in young leaves was an important limiting factor for photosynthetic CO_2 assimilation.

The results related to the gas exchange parameters showed that during leaf development in *E. japonicus*, the P_n and G_s increased in a similar manner during leaf expansion, while the C_i significantly decreased (Fig. 2). According to the criteria of Farquhar and Sharkey (1982), the lower P_n in young leaves was mainly caused by mesophyll factors rather than by lower stomatal conductance during leaf development. The mesophyll factors include the activity of enzymes associated with the Calvin cycle and the activities of light absorption and conversion by PSI and PSII.

The chlorophyll *a* fluorescence transient (O-J-I-P curve) has become one of the most useful tools in the study of PSII behavior, as the results reflect the structure and function of the PSII (Strasser, 1997). Jiang et al. (2006b) and Gao et al. (2014) observed that during leaf development in *Ulmus pumila* and *Malus micromalus*, the chlorophyll fluorescence transient changed remarkably. Recently, 820-nmreflection kinetics have been used to study PSI activity (Zhang et al., 2011; Strasser et al., 2010). The $\triangle I/I_O$ calculated from the 820-nm reflection has been widely used as an index of the content of active PSI reaction centers (Kim et al., 2001; Strasser et al., 2010; Zhang et al., 2011).

The present results demonstrated that during the development of *E. japonicus* leaves, the PSII activity increased more rapidly than did the PSI activity, which was supported by the observation that the ratio of

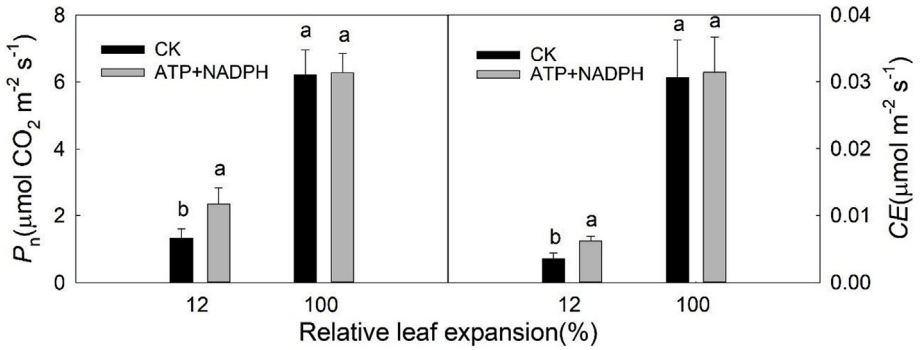

Fig. 8. The effect of applying exogenous assimilatory power (100 μM ATP, 50 μM NADPH) on photosynthesis in the youngest and fully expanded leaves. The measurements were performed after 1 h of treatment under saturated light (1200 μmol m^{-2} s^{-1}) and 400 μmol mol^{-1} CO_2.

PSII activity to PSI activity was highest in newly expanding leaves and decreased significantly with leaf expansion (Fig. 6). The coordination of PSII and PSI in plants ensures efficient electron transport. The lower activity of PSI compared to PSII in young leaves limits the linear electron transport and cyclic electron transport. The ETR was lowest in the young leaves, implying that the electron transport was severely inhibited from PSII to PSI.The F_v'/F_m' did not change much during development, but the q_P changed significantly; these results indicated that the lower ETR in the young leaves was caused by the more severe closing of active reaction centers, which may result from the lower PSI activity. The analysis of the expression levels of the PSI and PSII core proteins and the observation that the PET of PSII was much higher than that of PSI in young leaves (Table 1) further support the above conclusion.

It has been widely accepted that the expression of photosynthetic core proteins reflects the extent of development of the photosynthetic apparatus (Vanoosten and Besford, 2010). In the current study, the lowest expression level of PsaA in the youngest leaves greatly affected the PSI function. However, the relative content of Rubisco was much higher than that of PSI and PSII. Rubisco is the rate-limiting enzyme of the Calvin cycle (Carmosilva et al., 2015). Maayan et al. (2008) observed that during olive leaf development, the content of Rubisco increased gradually. Bertamini and Nedunchezhian (2002) noted that Rubisco activity in grapevine leaves was correlated with leaf age. Although the relative expression level of Rubisco was highest in the youngest leaves, the ratio of the *CE* and RuBP maximum regeneration rate in the young leaves to the fully expanded leaves were much lower than that of the Rubisco relative content. According to the above mentioned results, we presume that the relative expression levels of photosynthetic core proteins were not positively correlated with P_n during the development of *E. japonicas* leaves.

The *CE* was correlated with Rubisco activity (Yang et al., 2008; Urban et al., 2012). The actual activity of Rubisco depends largely on the activity of Rubisco activase (Portis, 2003), and Rubisco activation requires the energy that is released by ATP hydrolysis (Zielinski et al., 1989; Portis et al., 2008). Streusand and Portis (1987) reported that "ATP from photophosphorylation may act either as a substrate or regulatory metabolite for Rubisco activase and lead to light-dependent Rubisco activation at physiological levels of CO_2 and RuBP" (Page 154). The Calvin cycle is strongly dependent on the RuBP regeneration rate, which is coupled with the maximum ETR (Rosenthal et al., 2011; Urban et al., 2012). NADPH is produced through linear electron transport; ATP is produced through both linear and cyclic electron transport (Yuri et al., 2004). If the PSI or PSII is insufficiently developed in the youngest leaves, the light reactions will not produce enough assimilatory power to meet the demands of the Calvin cycle. Although the expression level of Rubisco in the youngest leaves was higher than that of the PSI and PSII, Rubisco was not fully activated due to the inadequate ATP production by the light reactions. It is reasonable to assume that the lower *CE* and CO_2 fixation in the youngest leaves might be strongly affected by the low ATP and NADPH supplied from the light reactions. The fact that P_n and *CE* remarkably increased with exogenous ATP and NADPH (Fig. 8) in the youngest leaves but not in the fully expanded leaves further supported this hypothesis. Therefore, we conclude that the slower development of PSI is an important factor limiting the P_n in young leaves of *E. japonicus*.

The current results suggest that PSI activity is likely the most important factor that limits photosynthesis during the development of the photosynthetic apparatus of *E. japonicus*. However, we cannot confirm whether plants that develop under different growth environments show similar patterns. Furthermore, many enzymes are involved in the Calvin cycle, in which several steps require ATP or NADPH as an energy source for reactions. In addition to Rubisco, other specific enzymes in the Calvin cycle are inhibited due to the inadequate supply of assimilatory power. Additional investigations are needed to clarify these details.

5. Conclusions

During the development of *E. japonicus* leaves, the expression content of the core protein was not positively correlated with the photosynthetic rate; the development speed of the PSI activity was lower than that of the PSII activity, which restricted the linear and cyclic electron transport and inhibited the production of ATP and NADPH. The inadequate supply of assimilatory power significantly inhibited the carboxylation efficiency and photosynthesis. The slower development of the PSI activity is one of the important limiting factors of photosynthesis during the development of *E. japonicus* leaves.

Conflicts of interest

The authors declare that they have no competing interests.

Author contributions

Qingming Li and Xin Zhong designed the research; Yuting Li and Xin Zhong performed all of the research, Xin Zhong and Huiyuan Gao wrote the article; Xingkai Che, Zishan Zhang and Shuhao Li performed the measurements of chlorophyll and gas exchange and analyzedthe data. All authors read and approved the final manuscript.

Acknowledgments

This work was financially supported by the National Natural Science Foundation of China (31872154, 31701966, 31771691, 31471918) and the Shandong Key Research and Development Plan (2017CXGC0201).

References

Bertamini, M., Nedunchezhian, N., 2002. Leaf age effects on chlorophyll, Rubisco, photosynthetic electron transport activities and thylakoid membrane protein in field grown grapevine leaves. J. Plant Physiol. 159, 799–803. https://doi.org/10.1078/0176-1617-0597.

Bongi, G., Mencuccini, M., Fontanazza, G., 1987. Photosynthesis of olive leaves: effect of light flux density, leaf age, temperature, peltates, and H_2O vapor pressure deficit on gas exchange. J. Am. Soc. Hortic. Sci. 112, 143–148. https://www.researchgate.net/publication/216356759.

Brandle, J.R., Campbell, W.F., Sisson, W.B., Caldwell, M.M., 1977. Net photosynthesis, electron transport capacity, and ultrastructure of *Pisum sativum* L. Exposed to ultraviolet-B radiation. Plant Physiol. 60, 165–169. https://doi.org/10.1104/pp.60.1.165.

Brestic, M., Zivcak, M., Kunderlikova, K., Sytar, O., Shao, H., Kalaji, H.M., Allakhverdiev, S.I., 2015. Low PSI content limits the photoprotection of PSI and PSII in early growth stages of chlorophyll b -deficient wheat mutant lines. Photosynth. Res. 125, 151–166. https://doi.org/10.1007/s11120-015-0093-1.

Carmosilva, E., Scales, J.C., Madgwick, P.J., Parry, M.A.J., 2015. Optimizing Rubisco and its regulation for greater resource use efficiency. Plant Cell Environ. 38, 1817–1832. https://doi.org/10.1111/pce.12425.

Çiçek, N., Oukarroum, A., Strasser, R.J., Schansker, G., 2018. Salt stress effects on the photosynthetic electron transport chain in two chickpea lines differing in their salt stress tolerance. Photosynth. Res. 136, 291–301. https://doi.org/10.1007/s11120-017-0463-y.

Farquhar, G.D., Caemmerer, S.V., Berry, J.A., 1980. A biochemical model of photosynthetic CO_2 assimilation in leaves of C_3 species. Planta 149, 78–90. https://doi.org/10.1007/BF00386231.

Farquhar, G.D., Sharkey, T.D., 1982. Stomatal conductance and photosynthesis. Annu. Rev. Plant Biol. 33, 317–345. https://doi.org/10.1146/annurev.pp.33.060182.001533.

Gao, J., Li, P., Ma, F., Goltsev, V., 2014. Photosynthetic performance during leaf expansion in Malus micromalus probed by chlorophyll a fluorescence and modulated 820 nm reflection. J. Photochem. Photobiol., B 137, 144–150. https://doi.org/10.1016/j.jphotobiol.2013.12.005.

Jia, Y.J., Cheng, D.D., Wang, W.B., Gao, H.Y., Liu, A.X., Li, X.M., Meng, Q.W., 2010. Different enhancement of senescence induced by metabolic products of Alternaria alternata in tobacco leaves of different ages. Physiol. Plantarum 138, 164–175. https://doi.org/10.1111/j.1399-3054.2009.01300.x.

Jiang, C.D., Shi, L., Gao, H.Y., Schansker, G., Toth, S.Z., Strasser, R.J., 2006a. Development of photosystems 2 and 1 during leaf growth in grapevine seedlings probed by chlorophyll a fluorescence transient and 820 nm transmission in vivo. Photosynthetica 44, 454–463. https://doi.org/10.1007/s11099-006-0050-5.

Jiang, C.D., Jiang, G.M., Wang, X., Li, L.H., Biswas, D.K., Li, Y.G., 2006b. Increased photosynthetic activities and thermos ability of photosystem II with leaf development of elm seedlings (*Ulmus pumila*) probed by the fast fluorescence rise OJIP. Environ. Exp. Bot. 58, 261–268. https://doi.org/10.1016/j.envexpbot.2005.09.007.

Jin, L., Che, X., Zhang, Z., Li, Y., Gao, H., Zhao, S., 2017. The mechanisms by which phenanthrene affects the photosynthetic apparatus of cucumber leaves. Chemosphere 168, 1498–1505. https://doi.org/10.1016/j.chemosphere.2016.12.002.

Kim, S.J., Lee, C.H., Hope, A., Chow, W.S., 2001. Inhibition of photosystems I and II and enhanced back flow of photosystem I electrons in cucumber leaf discs chilled in the light. Plant Cell Physiol. 42, 842–848. https://doi.org/10.1093/pcp/pce109.

Maayan, I., Shaya, F., Ratner, K., Mani, Y., Lavee, S., Avidan, B., Shahak, Y., Ostersetzer, Biran, O., 2008. Photosynthetic activity during olive (Olea europaea) leaf development correlates with plastid biogenesis and Rubisco levels. Physiol. Plantarum 134, 547–558. https://doi.org/10.1111/j.1399-3054.2008.01150.x.

Mahmood, T., Yang, P.C., 2012. Western blot: technique, theory and trouble shooting. N. Am. J. Med. Sci. 4, 429–434. https://dx.doi.org/10.4103%2F1947-2714.100998.

Maxwell, K., Johnson, G.N., 2000. Chlorophyll fluorescence—a practical guide. J. Exp. Bot. 51, 659–668. https://doi.org/10.1093/jexbot/51.345.659.

Portis Jr., A.R., 2003. Rubisco activase-Rubisco's catalyticchaperone. Photosynth. Res. 75, 11–27. https://doi.org/10.1023/A:1022458108678.

Portis Jr., A.R., Li, C., Wang, D., Michael, E. Salvucci, 2008. Regulation of Rubisco activase and its interaction with Rubisco. J. Exp. Bot. 59, 1597–1604. https://doi.org/10.1093/jxb/erm240.

Porra, R.J., 2002. The chequered history of the development and use of simultaneous equations for the accurate determination of chlorophylls a and b. Photosynth. Res. 73, 149–156. https://doi.org/10.1023/A:1020470224740.

Rosenthal, D.M., Locke, A.M., Khozaei, M., Raines, C.A., Long, S.P., Ort, D.R., 2011. Over-expressing the C_3 photosynthesis cycle enzyme Sedoheptulose-1-7 Bisphosphatase improves photosynthetic carbon gain and yield under fully open air CO_2 fumigation (FACE). BMC Plant Biol. 11, 123. https://doi.org/10.1186/1471-2229-11-123.

Salvatori, E., Fusaro, L., Gottardini, E., Pollastrini, M., Goltsev, V., Strasser, R.J., Bussotti, F., 2014. Plant stress analysis: application of prompt, delayed chlorophyll fluorescence and 820nm modulated reflectance. Insights from independent experiments. Plant Physiol. Biochem. 85, 105–113. https://doi.org/10.1016/j.plaphy.2014.11.002.

Satoh, K., Koike, H., Ichimura, T., Katoh, S., 1992. Binding affinities of benzoquinones to the Q_B site of Photosystem II in Synechococcus oxygen-evolving preparation. BBA-Bioenergetics 1102, 45–52. https://doi.org/10.1016/0005-2728(92)90063-8.

Strasser, B.J., 1997. Donor side capacity of Photosystem II probed by chlorophyll a fluorescence transients. Photosynth. Res. 52, 147–155. https://doi.org/10.1023/a:1005896029778.

Strasser, R.J., Srivastava, A., Tsimilli, Michael, M., 2000. The fluorescence transient as a tool to characterize and screen photosynthetic samples. In: Mohammad, Y. (Ed.), Probing Photosynthesis. CRC Press, England, pp. 445–483. https://www.researchgate.net/publication/252250818.

Strasser, R.J., Tsimilli-Michael, M., Qiang, S., Goltsev, V., 2010. Simultaneous *in vivo* recording of prompt and delayed fluorescence and 820-nm reflection changes during drying and after rehydration of the resurrection plant *Haberlea rhodopensis*. BBA-Bioenergetics 1797, 1313–1326. https://doi.org/10.1016/j.bbabio.2010.03.008.

Streusand, V.J., Portis, A.R., 1987. Rubisco activase mediates ATP-dependent activation of ribulose bisphosphate carboxylase. Plant Physiol. 85, 152–154. https://doi.org/10.1104/pp.85.1.152.

Tanaka, K., Gilroy, S., Jones, A.M., Stacey, G., 2010. Extracellular ATP signaling in plants. Trends Cell Biol. 20, 601–608. https://doi.org/10.1016/j.tcb.2010.07.005.

Tonón, C., Terrile, M.C., Iglesias, M.J., Lamattina, L., Casalongué, C., 2010. Extracellular ATP, nitric oxide and superoxide act coordinately to regulate hypocotyl growth in etiolated Arabidopsis seedlings. J. Plant Physiol. 167, 540–546. https://doi.org/10.4161/psb.5.6.11579.

Urban, O., Hrstka, M., Zitová, M., Holišová, P., Šprtová, M., Klem, K., Calfapietra, C., Angelis, P.D., Marek, M.V., 2012. Effect of season, needle age and elevated CO_2 concentration on photosynthesis and Rubisco acclimation in *Picea abies*. Plant Physiol. Biochem. 58, 135–141. https://doi.org/10.1016/j.plaphy.2012.06.023.

Vanoosten, J.J., Besford, R.T., 2010. Some relationships between the gas exchange, biochemistry and molecular biology of photosynthesis during leaf development of tomato plants after transfer to different carbon dioxide concentrations. Plant Cell Environ. 18, 1253–1266. https://doi.org/10.1111/j.1365-3040.1995.tb00185.x.

Yang, W.J., Chen, H.F., Zhu, F.Y., Hu, M.Q., Jiang, D.A., 2008. Low concentration of bisulfite enhances photosynthesis in tea tree by promoting carboxylation efficiency in leaves. Photosynthetica 46, 615–617. https://doi.org/10.1007/s11099-008-0103-z.

Yuri, M., Mihoko, H., Chikahiro, M., Ken-ichi, T., Tsuyoshi, E., Masao, T., Toshiharu, S., 2004. Cyclic electron flow around photosystem I is essential for photosynthesis. Nature 429, 579–582.

Zhang, Z., Jia, Y., Gao, H., Zhang, L., Li, H., Meng, Q., 2011. Characterization of PSI recovery after chilling-induced photoinhibition in cucumber (*Cucumis sativus* L.) leaves. Planta 234, 883–889. https://doi.org/10.1007/s00425-011-1447-3.

Zielinski, R.E., Werneke, J.M., Jenkins, M.E., 1989. Coordinate expression of Rubisco activase and Rubisco during barley leaf cell development. Plant Physiol. 90, 516–521. https://doi.org/10.1104/pp.90.2.516.